

T2  
3  
3

MIT LIBRARIES



3 9080 02993 0119

V393  
.R468

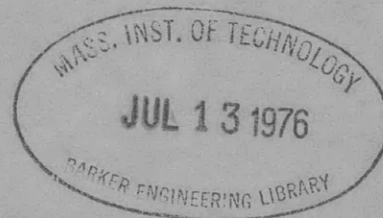
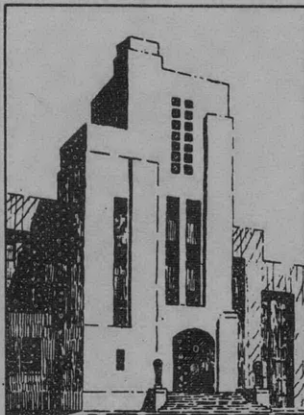
#3

NAVY DEPARTMENT  
THE DAVID W. TAYLOR MODEL BASIN  
WASHINGTON 7, D.C.

INFLUENCE OF REYNOLDS NUMBER ON  
THE SEPARATION (CAVITATION) FLOW

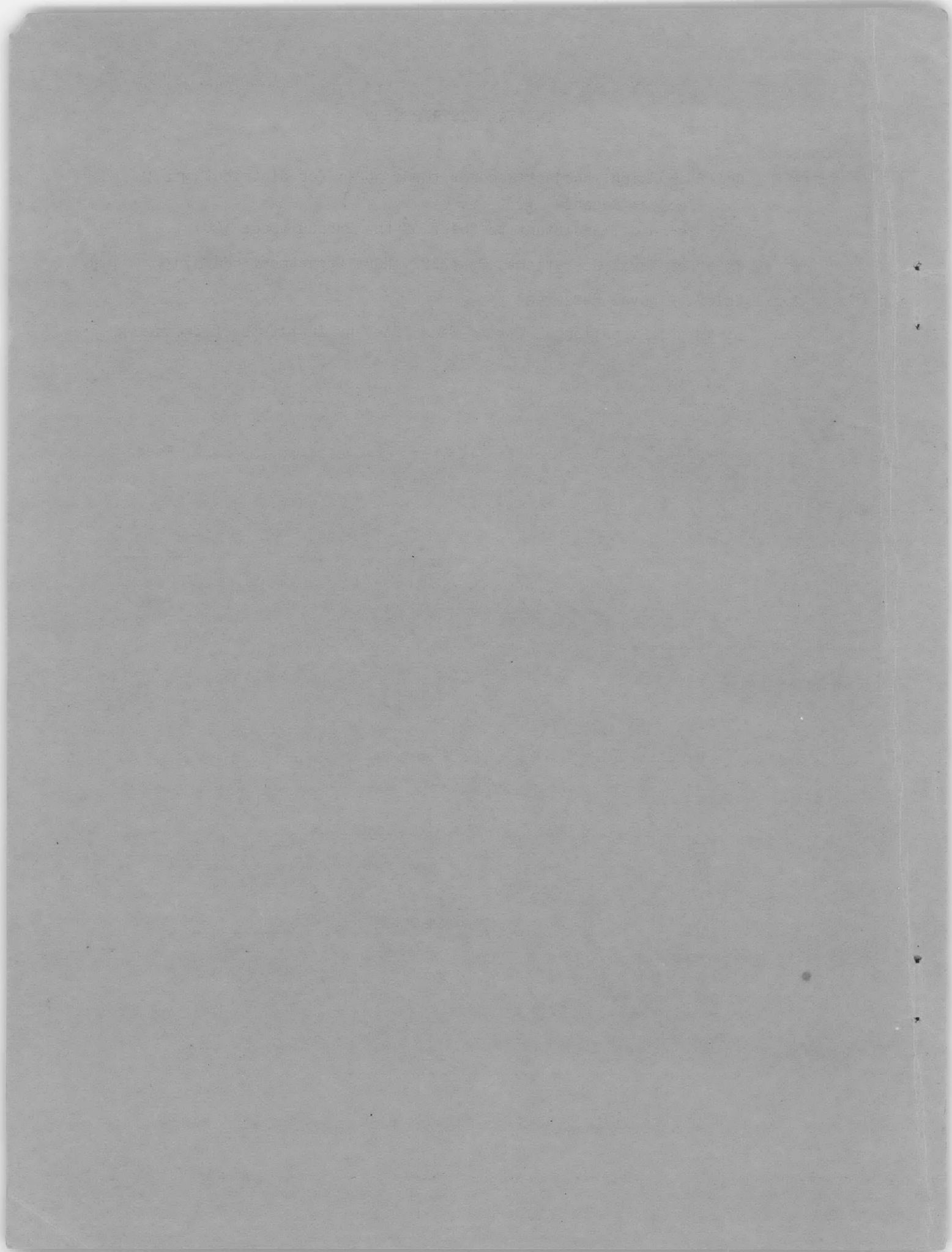
by

V.A. Konstantinov



November 1950

Translation 233



INITIAL DISTRIBUTION

Copies

- 6 Chief BuShips, Project Records (Code 362), for distribution:
  - 3 Project Records
  - 1 Technical Assistant to Chief of the Bureau (Code 106)
- 2 Chief of Naval Operations, Op-322F2, Navy Department, Washington, D.C.
- 2 Chief of Naval Research
- 1 Director, Experimental Towing Tank, Stevens Institute of Technology,  
711 Hudson Street, Hoboken, N.J.
- 1 Comdr. G.C. Manning (CC) USN (Ret.) Department of Naval Architecture  
and Marine Engineering, Massachusetts Institute of Technology,  
Cambridge 39, Mass.
- 1 Prof. Frank M Lewis, Department of Mechanical Engineering, Massa-  
chusetts Institute of Technology, Cambridge 39, Mass.



INFLUENCE OF REYNOLDS NUMBER ON THE SEPARATION (CAVITATION) FLOW

(Vliianie Chisla Reynoldsa na Otryvnoe Obtekanie)

by

V.A. Konstantinov

Izvestia Akademii Nauk SSSR, Otdelenie Tekhnicheskikh Nauk, 1946,  
No. 10, pp. 1355-1373

Translated by G. Weinblum, D. Eng.

November 1950

Translation 233

## TABLE OF CONTENTS

	Page
INTRODUCTION . . . . .	1
SHORT DESCRIPTION AND MAIN CHARACTERISTICS OF THE CAVITATION TUNNEL .	1
EXPERIMENTAL METHODS . . . . .	3
PERFORMANCE OF EXPERIMENTS AND RESULTS . . . . .	6
ANALYSIS OF OBTAINED RESULTS . . . . .	10
CONCLUSIONS . . . . .	19

## INTRODUCTION

Problems of flows with separation and cavitation are today of great importance, especially for high-speed ships.

Notwithstanding the fact that more than half a century has gone by since the discovery of cavitation, the physical character and even problems of practical importance like the criterion of similitude have not yet been wholly studied. We find publications on special questions only; experimental investigations are rare and systematic series are lacking.

Experimental work is urgently needed at present, as it should furnish data for the development of theory and further studies of various phenomena.

The present investigation is a first task in this direction and of rather tentative character. Because of the somewhat inadequate facilities and lack of systematic experience, the author has confined himself primarily to the qualitative side of the problem. The finding of exact quantitative results is connected with inherent difficulties even when perfect facilities are available; the solution of these difficulties is the subject of a special investigation.

However a comparison of our results with data published by other laboratories indicates that even quantitative agreement may be sufficient in cases where no great accuracy is needed.

As long as the influence of the type of tunnel, the character of flow (for instance, degree of turbulence), and other unknown factors have not been investigated, every laboratory can assert with equal right that its data are the most exact. To enable an objective judgment on the accuracy of the present research, we mention the factors which to a certain degree may have influenced the exactness of experiments.

We hope that the present investigation will form a modest contribution to a new branch of science—the hydromechanics of flows with separation, founded by the work of W.L. Posdunine.

## SHORT DESCRIPTION AND MAIN CHARACTERISTICS OF THE CAVITATION TUNNEL

Under war conditions the erection of a new cavitation tunnel met with difficulties; it was therefore decided to adapt the existing pressure arrangement at the Laboratory for Physical Hydrodynamics of the Academy of U.S.S.R. by some rebuilding, which was basically finished in 1943. The scheme is given in Figure 1.

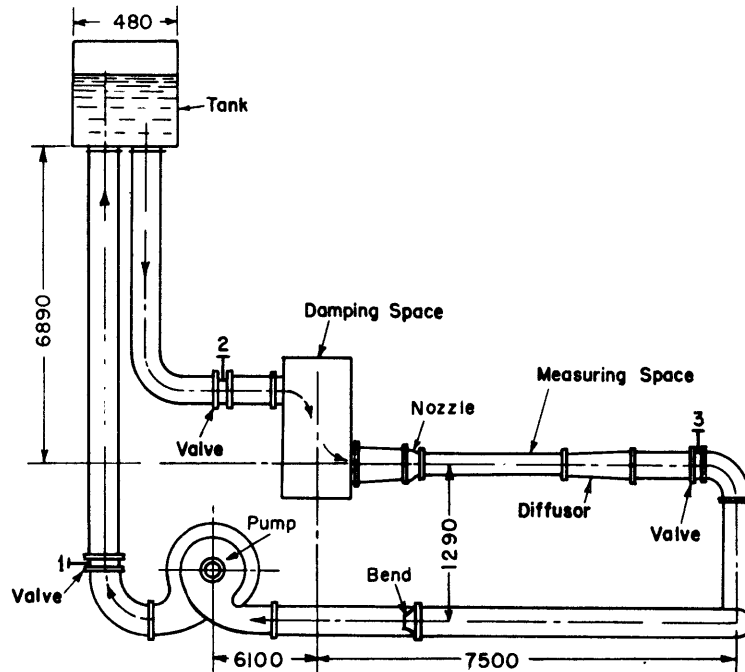


Figure 1 - General Scheme of the Cavitation Arrangement at the Institute of Mechanics of the Academy of Science (A S.) U S.S.R.

The final adaptation was performed during 1944, so that it was possible to make some simple experiments at the end of the year.

From Figure 1 it appears that the tunnel represents a closed system; the water circulation is realized by a pump (6) with an effective output of 175 liters/sec. driven by a synchronous motor of 55 kw at 730 rpm.

The working section (4) has the dimensions 70 x 200 mm; it consists of two metallic horizontal beams forming the skeleton and two vertical frames filled with glass windows. One of the frames is made of two parts between

which a metallic plate (Figure 2) is inserted; the plate bears a moveable appliance on which the models can be fastened. This appliance is fitted with an indicator scale so that the bodies may be fixed at a definite angle with respect to the stream. The turning device is designed in such a way that tubes for pressure measurements on the surface of the bodies can be installed.

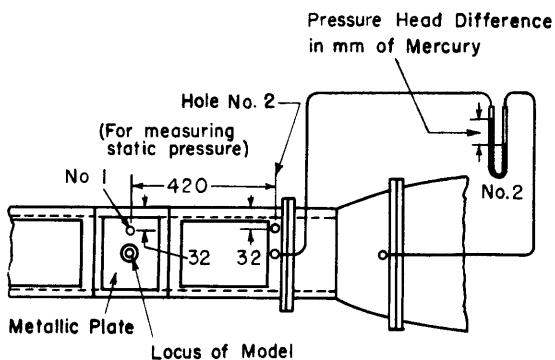


Figure 2



The working part is made of such length (1.9 m) that the cavity formed behind the body by separation can be observed. The measuring apparatus can be attached by seven bolts screwed into the fundamental beam.

In front of the testing length a Witoczynski nozzle system (3) is arranged with a coefficient of contraction of 4.2; at the rear is a diffusor (5) with a length of 1 m and an opening angle of  $3^\circ$ .

The speed regulation is performed by a valve (7) which in principle one should be able to operate over a wide range; in fact, the lower limit is given by the behavior of the pump which starts to work irregularly when strongly throttled.

The basic data of the tunnel are: Greatest speed on the axis of the testing section 15 m/s, lowest speed 4 m/s, lowest cavitation number  $\sigma = 0.65$ .

#### EXPERIMENTAL METHODS

The most important and difficult problem when experimenting is the determination of the average speed. From the present viewpoint it is essential to know the velocity distribution over the working section for a number of working conditions covering a sufficiently wide range. It proved to be difficult to perform this extensive work under the existing inadequate conditions of the installation. On the other hand the correctness of the present method in determining the average speed may be questioned, especially when a great part of the working section is obstructed—as is true in the present case and generally in cavitation experiments.

Usually the velocity distribution is measured without the model. The latter causes a considerable blocking effect, which was for the first time stated at the NACA laboratory. The true nature of the necessary correction to allow for this effect is not yet known.

Under conditions of cavitation a number of special problems arise: e.g., 1, how is the measurement of speed influenced by the cavitation of the Prandtl-tube itself, 2, should we refer the narrowing of the flow caused by the body to the actual section of the body or to the maximum section of the cavity?

These difficulties induced us to give up the determination of the velocity field, having in mind that the primary aim of our work did not consist of getting quantitative results.

The necessary average speed was found by measuring the output. Using this average velocity some cylinders with different diameters were tested in normal flow; the results represented in Figure 3 indicate that the agreement is quite satisfactory as long as we confine ourselves to the qualitative

part of the phenomena. It is intended to continue the experiments to get more accurate quantitative data but only when the experimental problems mentioned above have been solved.

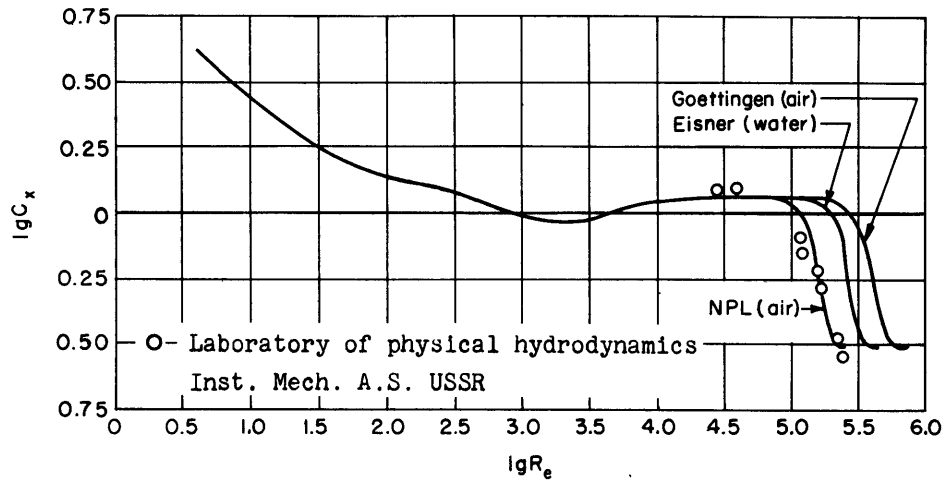


Figure 3

During the experiments the velocity on the axis of the tube was determined from the pressure drop in the contraction nozzle, Figure 2, after having checked it by a Prandtl-tube installed at the place of the model. The calibration curve is represented in Figure 4.

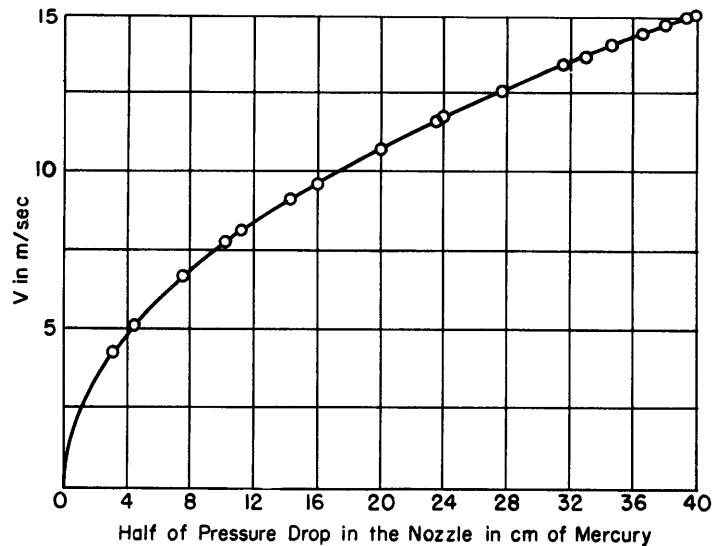


Figure 4 - Curve for Determining Velocity as Function of Pressure Drop in the Nozzle

The pressure on the cylinder was determined with respect to the static pressure at Hole Number 2, Figure 2, and was immediately read off the manometer differentially connected with the cylinder and the mentioned hole; three experiments were made to check if the installation of the cylinder influenced the static pressure first without a cylinder, then with the cylinders of 33 mm and 50 mm diameter; no influence could be found. The resulting curves are represented in Figure 5.

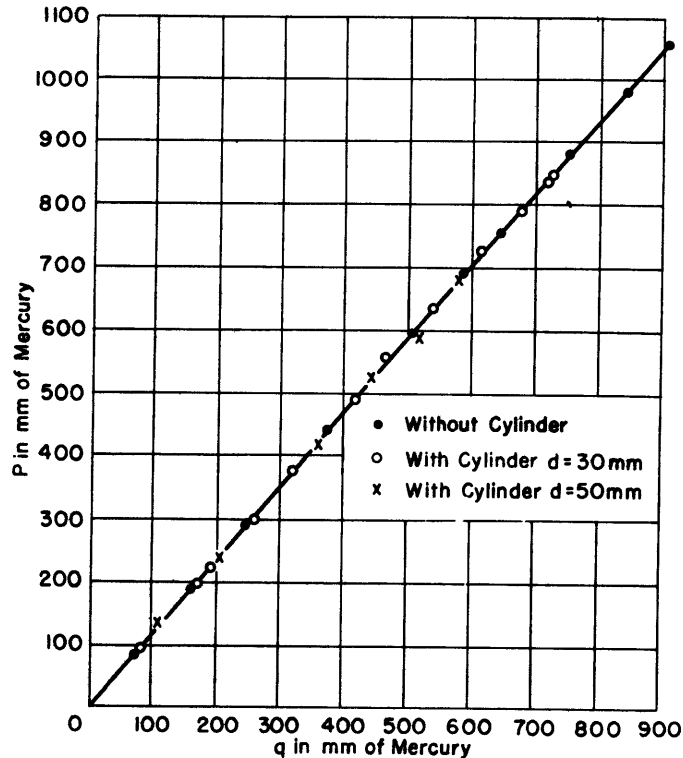


Figure 5 - Calibration of Static Pressure at Point Number 2

Further, losses which occurred between the tank and the locus of the model (Section 1, Figure 2) were measured with the aim of calculating the static pressure of the undisturbed flow at this place by the formula

$$P_{\infty} = P_{\text{barometer}} + Z - h_{\text{losses}} - q_{\infty} \quad [1]$$

where  $Z$  is the depth of immersion of the model with respect to the level of the tank,

$h_{\text{losses}}$  is the losses between tank and model, and

$q_{\infty} = KK_1^2 \frac{\rho V^2}{2}$  is the velocity head of the undisturbed flow.

Here K is the correction for the nonuniform speed distribution over the section (K is assumed  $\cong 1$ )

$K_1 = \frac{L}{L - d}$  is the coefficient which takes account of the influence of the boundaries of the flow, and

L is the dimension of the section measured perpendicularly to the axis of the cylinder with the diameter d.

When computing the pressure on the cylinder a correction was used equaling the difference between the static pressure at Hole Number 2 (Figure 2) and the result of Formula [1].

#### PERFORMANCE OF EXPERIMENTS AND RESULTS

Six circular cylinders with the diameters 5, 10, 20, 30, 40, and 50 mm were tested.

Instead of using scales the resistance of the cylinders was derived from pressure measurements on the cylinders. This method has some advantages compared with weighing as it gives us the physical reasons for changes of resistance.

For pressure measurements a 0.5 mm hole was bored in the mid-section of each cylinder; this hole meets a canal drilled along the axis which by a rubber tube was connected with the manometer. The cylinder was fastened on the turning disc fitted with an arm, so that the hole could be fixed at any desired angle relative to the flow. By symmetry, measurements were made between  $0^\circ$  and  $180^\circ$  at intervals of  $10^\circ$ . The second leg of the manometer is connected with Hole Number 2 (Figure 2). Thus manometer readings give the pressure on the cylinder with respect to the static pressure in this hole; as the cylinder was located at Section 1, we corrected manometer readings by the difference of static pressure at Holes 2 and 1.

The pressure coefficient was computed by the formula

$$\mathcal{N} = \frac{(P_m - P_2) + (P_2 - P_\infty)}{q_\infty} \quad [2]$$

where  $P_m - P_2$  is the immediate manometer readings and  $P_2 - P_\infty$  is the indicated correction ( $P_2$  taken from the curve, Figure 5,  $P_\infty$  calculated by Formula [1]). The resistance coefficient of the cylinders was calculated from

$$C_x = \int_0^\pi \mathcal{N} \cos \phi \, d\phi \quad [3]$$

where  $\phi$  is the angle at the center between the radius drawn through the hole on the cylinder and the direction of the flow. The integration was performed graphically.

The pressure results are shown in Figures 6 through 11. Final results are given in Figure 12, as

$$C_x = f(\sigma) \quad .$$

where  $\sigma = \frac{P_\infty - P_d}{q_\infty}$ , and in Table 1.

The accuracy of the present experiments may have been influenced by:

1. Cavitation of the Prandtl tube; the tube should be checked in cavitating conditions.

2. Determination of static pressure of a section from measurements in one hole only is not reliable; we should use more holes connected by a collector.

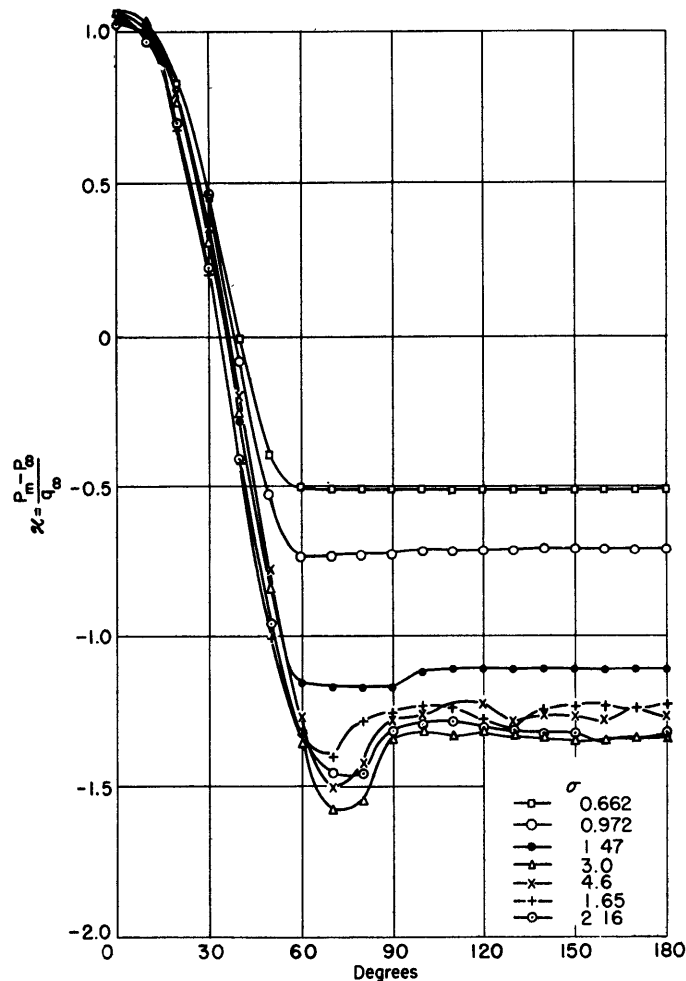


Figure 6 - Pressure Distribution on the Cylinder  $d = 5$  mm. for Different Conditions of Flow

3. At the beginning of the experiments insufficient care was used to avoid air in the manometer tube; that is the reason for a more pronounced scattering of points corresponding to cylinders of 40 and 50 mm diameter (Figure 12) which were tested first.

Later after each experiment the cylinder was turned back to the initial position without stopping the flow and the readings of the manometer were checked; in cases of disagreement the experiment was cancelled. In addition, observations were made after the experiments were completed and the flow had been stopped to see that the manometer reached its zero point.

However, the above-mentioned factors have not influenced results too much, as was checked by other results obtained in the VIGM Laboratory (Federal Institute of Hydraulic Machines).

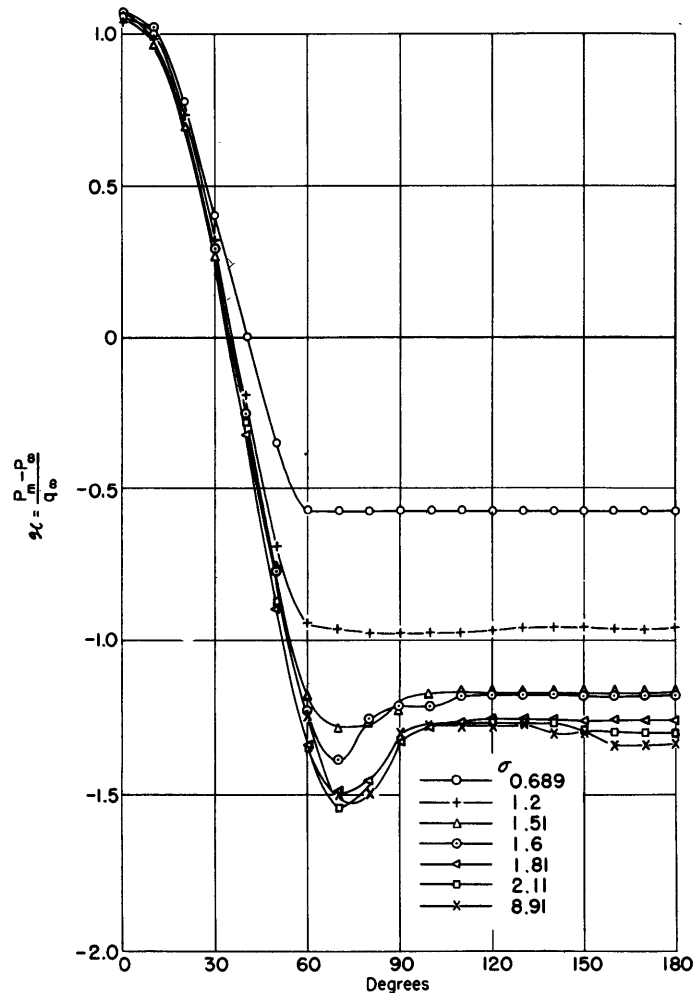


Figure 7 - Pressure Distribution on the Cylinder  $d = 10$  mm for Different Conditions of Flow

TABLE 1

Protocol Number	d Cylinder mm	v Average Velocity m/sec	$\sigma$	$R_e$	$C_x$	Remarks
47	5	13.03	0.662	650,000	0.845	Cavity (length) 10 diameters
48	5	12.21	0.932	41,000	0.972	Cavity (length) 5 diameters
49	5	10.98	1.47	38,100	1.210	Cavity (length) 2 diameters
54	5	10.6	1.65	63,100	1.26	Cavity (length) 2 diameters
55	5	10.2	1.89	64,000	1.28	Cavity (length) about 1.5 diameters
56	5	9.78	2.16	63,000	1.285	Cavity (length) about 1.5 diameters
50	5	8.75	3.00	31,250	1.38	Hardly noticeable beginning of cavitation
51	5	7.48	4.6	27,300	1.344	Weak noise indicating cavitation
17	10	13.00	0.689	78,500	0.889	Cavity 10 diameters
61	10	11.55	1.2	75,000	1.1	Cavity 3 diameters
18	10	10.91	1.51	68,700	1.224	Cavity 2 diameters
57	10	10.70	1.6	63,600	1.265	Cavity about 1.5 diameter
58	10	10.33	1.81	62,600	1.280	Cavity about 1.5 diameter
59	10	9.90	2.11	62,200	1.3	Beginning cavitation
19	10	5.66	8.97	38,000	1.33	Without cavitation
62	20	13.10	0.646	162,000	0.847	Full separation
63	20	12.5	0.898	154,300	0.954	Cavity 5 diameters
64	20	11.93	1.030	147,000	1.03	Cavity 2.5 diameters
65	20	11.4	1.25	132,000	1.125	Cavity about 1.5 diameter
66	20	10.98	1.44	141,500	1.215	Cavity about 1.25 diameter
67	20	10.32	1.78	136,000	1.28	Cavity about 0.5 diameter with interruptions
75	20	9.83	2.12	117,000	1.06	Clear start of cavitation
76	20	9.11	2.67	112,500	1.052	Beginning of weak cavitation phenomena
16	30	13.12	0.703	230,000	0.868	Full separation
68	30	12.59	0.821	222,000	0.92	Cavity 3 diameters
69	30	11.85	1.084	214,000	1.077	Cavity 2 diameters
70	30	11.38	1.28	209,000	1.17	Cavity about 1.25 diameter
71	30	10.72	1.59	202,000	1.24	Cavity about 0.5 diameter
72	30	10.39	1.79	202,000	0.882	Beginning cavitation
73	30	10.00	2.1	179,000	0.765	Clear beginning of cavitation
74	30	9.7	2.24	183,000	0.775	Beginning of slight cavitation phenomena
35	40	13.22	0.692	310,000	0.792	Full separation
36	40	12.97	0.771	314,000	0.857	Cavity 3 diameters
38	40	12.2	1.02	286,500	1.043	Cavity about 1.5 diameter
39	40	11.68	1.23	283,000	1.128	Cavity about 1 diameter
32	40	11.41	1.355	294,000	1.20	Cavity about 1 diameter
40	40	10.94	1.55	275,000	1.295	Cavity about 0.5 diameter
45	40	10.93	1.57	280,000	1.25	Cavity about 0.25 diameter
44	40	10.78	1.65	271,000	0.662	Beginning cavitation, separate sound development
43	40	10.55	1.772	251,000	0.602	Beginning cavitation
41	40	10.10	2.03	262,000	0.602	Beginning cavitation
42	40	9.43	2.5	248,000	0.532	Weak noise indicating cavitation
29	40	7.00	5.57	168,600	0.532	Weak noise indicating cavitation
28	40	4.84	12.95	113,800	0.839	Without cavitation
24	50	13.33	0.68	432,000	0.813	Full separation
23	50	12.70	0.868	400,000	0.943	Cavity 2 diameters
21	50	12.02	1.11	355,000	1.03	Cavity 1 diameter
25	50	10.5	1.84	321,000	0.331	Clear beginning of cavitation
26	50	9.5	2.5	300,000	0.332	Weak noise indicating cavitation
22	50	7.55	4.58	229,000	0.297	Without cavitation
27	50	4.88	12.75	158,600	0.628	Without cavitation

As long as we are not able to find the speed equivalent to the speed of a free stream, when dealing with cavitation phenomena, some doubts as to the accuracy of the results obtained will remain. That is the most difficult and important problem not yet solved at present.

#### ANALYSIS OF OBTAINED RESULTS

Observing Figure 12, which shows the result of experiments with different cylinders at different Reynolds numbers as a function of the cavitation parameter, we see two regions divided by a quite pronounced jump in the resistance coefficient. This jump indicates a certain fundamental change in flow around the body; therefore we call the corresponding cavitation number a critical number, by analogy with Reynolds number, when dealing with a cavitation free flow.

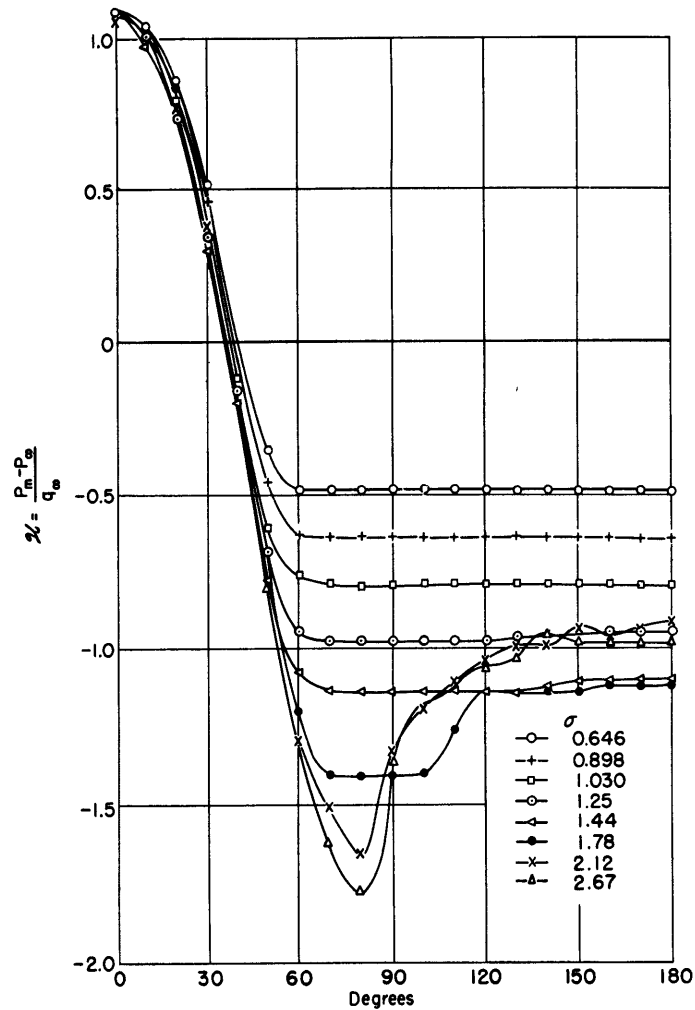


Figure 8 - Pressure Distribution on the Cylinder  $d = 20$  mm for Different Conditions of Flow



The region to the right of the jump we name "undercritical" and to the left—"supercritical;" we shall use this terminology further and shall give the reasons for its introduction.

The undercritical region which, by the former terminology, corresponds to the initial state of cavitation, is characterized by a very small change of the resistance coefficient  $C_x$  for a fixed range of  $R$  and, on the contrary, by a very pronounced variation of this coefficient (up to 4 times) when the range of  $R$  is changed (Figure 12). Thence, contrary to the existing opinion, it is more important to comply with  $R$  than with the coefficient  $\sigma$  when performing model research at the initial or not wholly developed state of cavitation. When we take the range of  $R$  beneath the critical point for flow without cavitation, no jump in the resistance for cavitating flow does occur, as it may be seen for the cylinders with 5 and 10 mm diameter. This

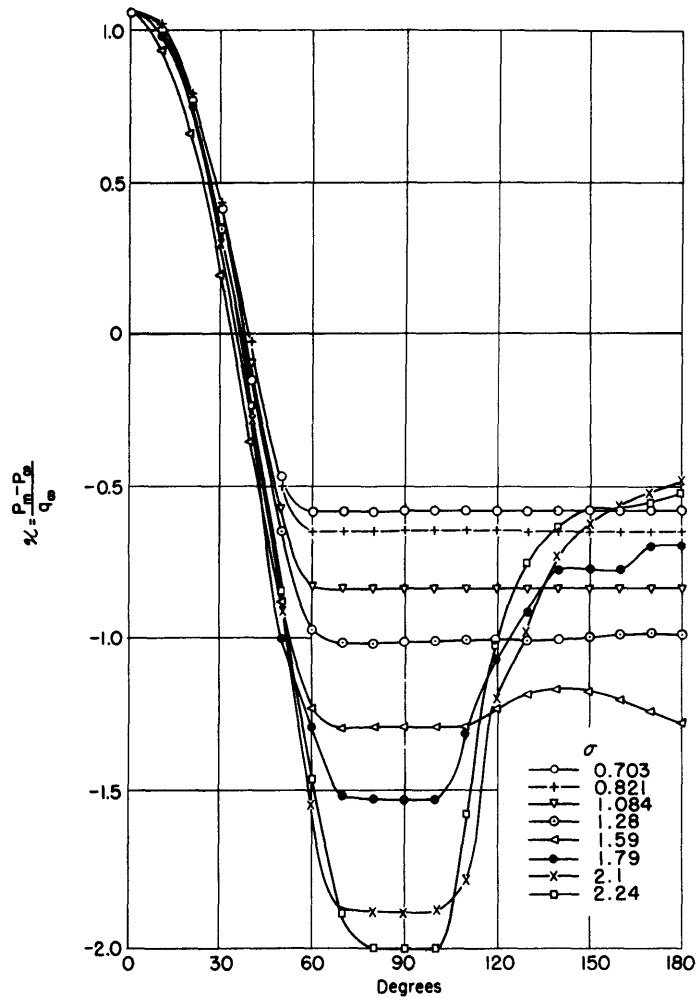


Figure 9 - Pressure Distribution on the Cylinder  $d = 30$  mm for Different Conditions of Flow

indicates a connection between the two phenomena and suggests further that no fundamental difference exists between a "normal" and a cavitating flow in the region of "undercritical" cavitation numbers. Judging by the resistance coefficient alone, it would be difficult to state that some processes are developing which distinguish the flow from the normal except for other phenomena, like local boiling of the liquid by separating gas and vapor, and erosion.

It may be interesting to substitute the erosion effect for the resistance coefficient and investigate the intensity of the former as functions of  $R$  and  $\sigma$ , as the practical importance of erosion may be not less than that of the increase in resistance

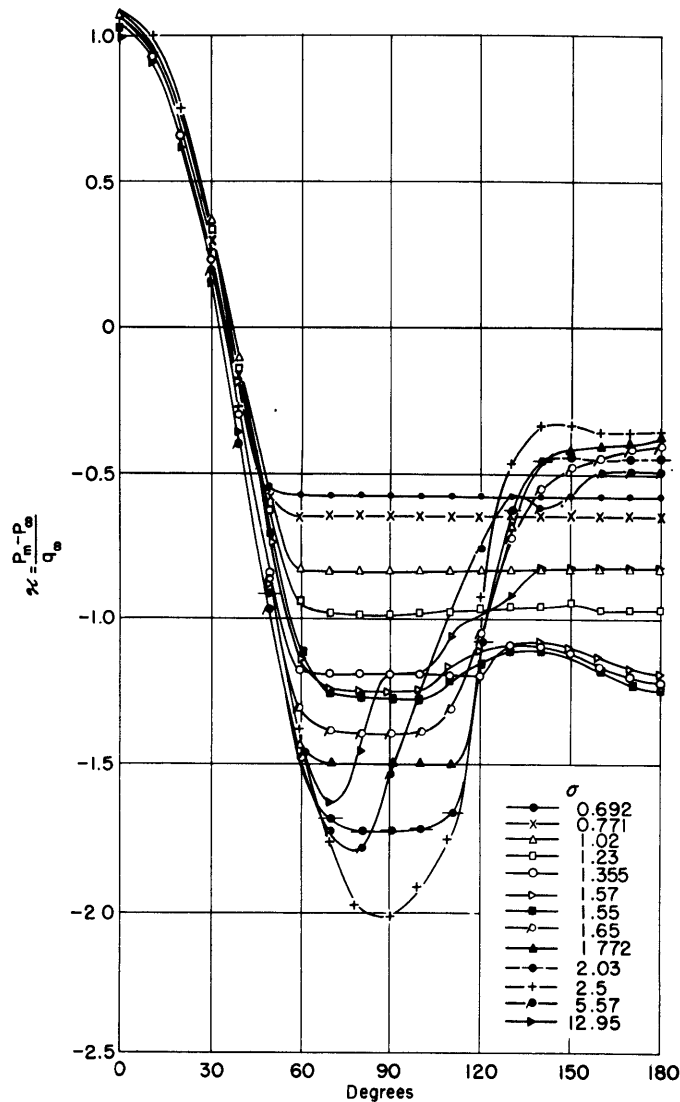


Figure 10 - Pressure Distribution on the Cylinder  $d = 40$  mm  
for Different Conditions of Flow

The supercritical range of cavitation presents quite a different picture. Although the interval of  $R$  is sufficiently wide (38,000 to 432,000) the experimental points form a comparatively narrow strip. That indicates only a slight dependence of the resistance coefficient on  $R$ , if any, in this region. To settle finally this question, we need additional and more exact experiments, although some data on this subject exist at present.

The supercritical region is characterized by a decreasing coefficient of resistance with decreasing  $\sigma$ , and apparently this decrease follows a linear law. However, this linear dependence was not obtained in all cases, a fact which may be explained by inaccuracy of experiments. In fact, the scattering of points should be much less; this was proved by repeated checking experiments performed at the VIGM Laboratory; the results are shown in Figure 13. These experiments seem to prove experimentally the hypothesis mentioned above that the coefficient  $C_x$  is independent of  $R$  in the supercritical region,

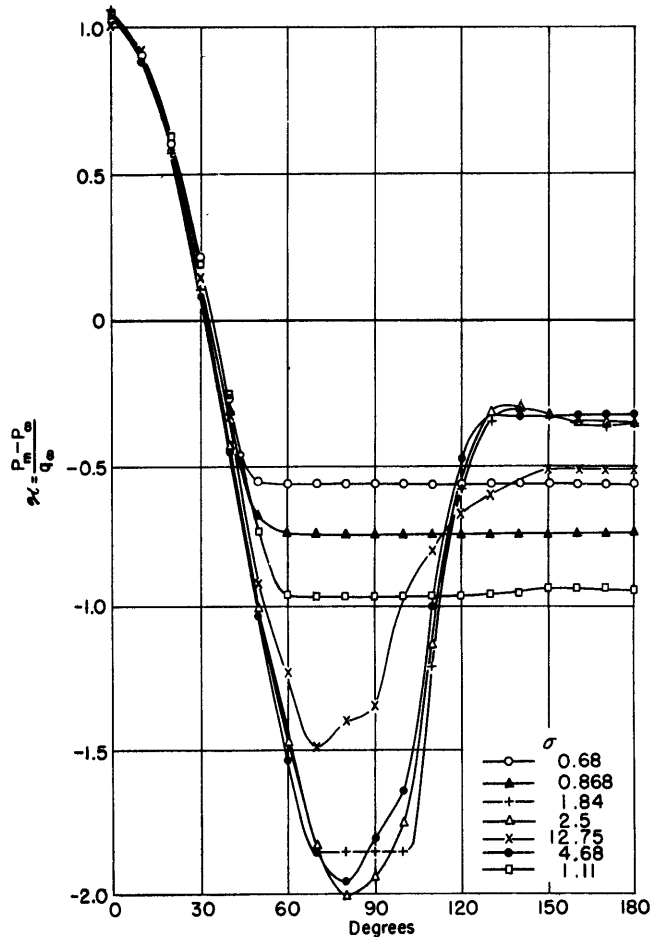


Figure 11 - Pressure Distribution on the Cylinder  $d = 50$  mm  
for Different Conditions of Flow

as the scattering of points is within the accuracy of experiments. But later experiments performed at the same laboratory make this statement doubtful, as may be seen from Figure 14. For comparison, in Figure 15 these results are represented in the same manner as Figure 13; here we observe an important scattering of points which cannot be explained by lack of accuracy.

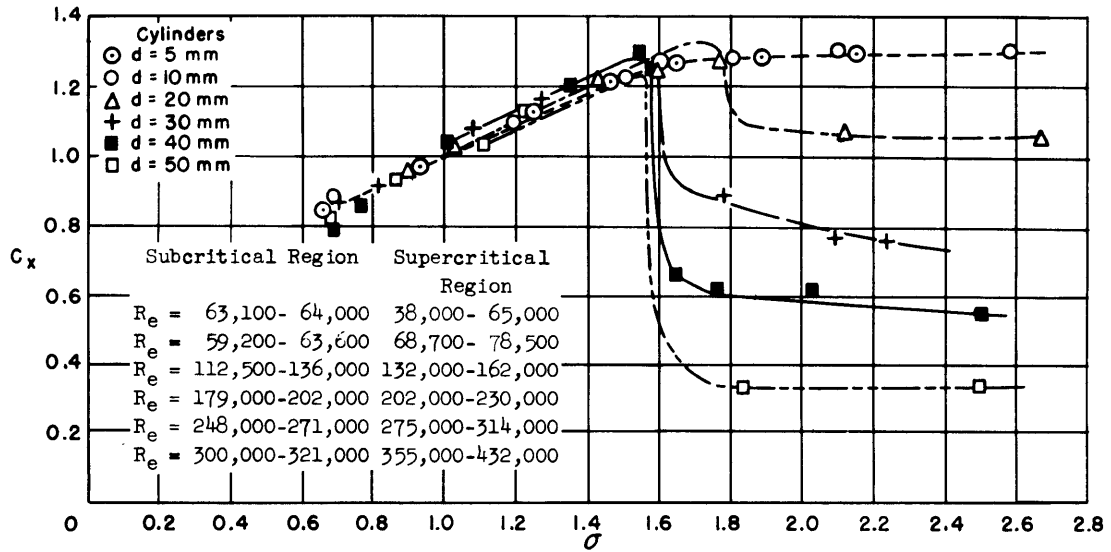


Figure 12

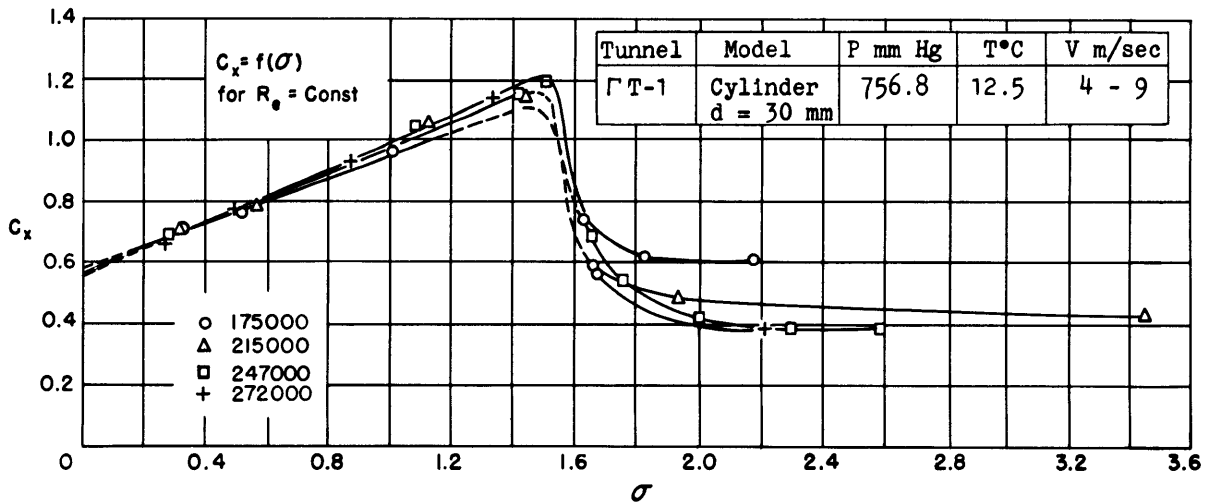


Figure 13

Returning to Figure 14, we see, besides a general decrease of  $C_x$  with growing  $R$ , quite pronounced steps just at points of the  $C_x$  curves which correspond to a change of cylinders with different diameters. This fact indicates the existence of an influence hitherto not yet considered, which, in our opinion, may be the variation in pressure during experiments and the

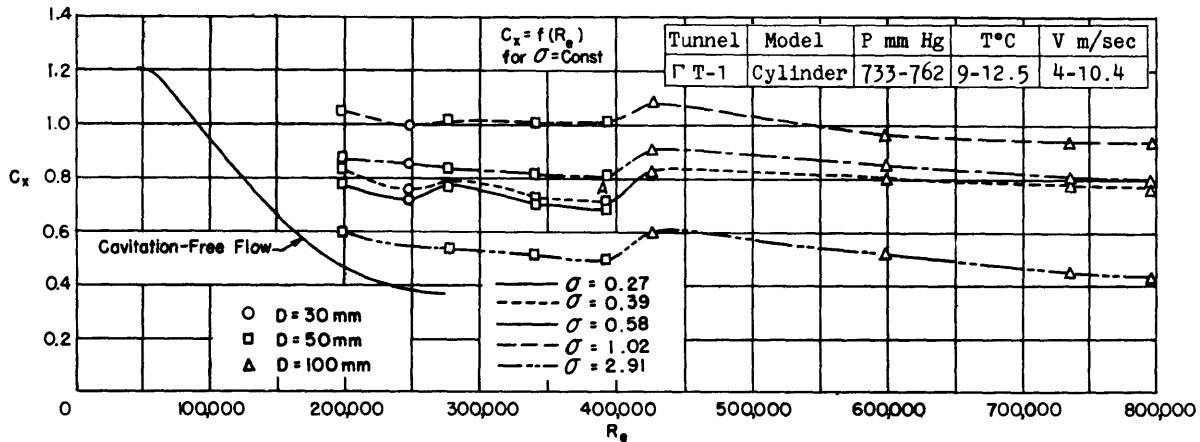


Figure 14

difference of air content in water due to this variation. It is known that the solubility of gases in water increases with increasing pressure, and vice versa. The curves (Figure 14) indicate that besides  $R$  other factors were varied; hence the question arises as to which may be the real causes of the change in the resistance coefficient  $C_x$ .

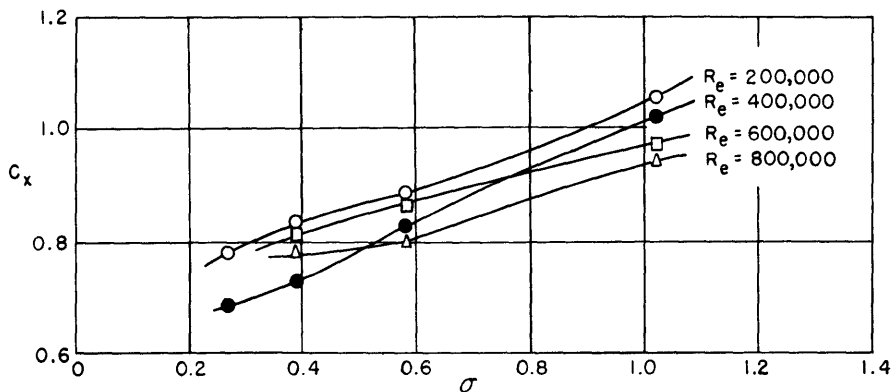


Figure 15

Take, for instance, the curve with the parameter  $\sigma = 0.39$  and observe its shape from left to right. For the given cylinder and value of  $R$  at the extreme left point of the curve we can reach the cavitating number 0.39 by a high vacuum only, which leads to a decrease of the air content. The next point of the curve has been obtained by a cylinder with a smaller diameter; that means the speed was considerably increased to get a higher  $R$  and obviously the pressure, too, causing an increase in air contents. The slope of the curve is downward. To get the next point the first cylinder was installed again, the speed and pressure were reduced; the air content drops and the

coefficient  $C_x$  increased. The following points were obtained for the same cylinder: Increase of velocity, pressure and air content, the curve  $C_x$  at the same time falling down to the point A where the limiting speed of the installation is reached. The further increase of  $R$  was performed by the larger cylinder ( $d = 100$  mm); velocity, pressure and air content were nearly the same as at the starting point, hence the coefficient  $C_x$  equals accurately the corresponding value at this point.

Next, experiments were performed by the same scheme up to the point at the right. This point is doubtful, however, as it should be on the same level as A (see, for instance, the curve  $\sigma = 0.58$ ), because all conditions—speed, pressure, air content—are the same at both points.

To avoid influence of air content, we should have used the same regime (speed, pressure) for a given  $\sigma$ , increasing Reynolds number  $R$  by increasing the diameters of cylinders only. We could then expect horizontal straight lines on Figure 14, which would prove the independence of  $C_x$  from  $R$  in the supercritical region.

Why did we not find such an influence of the air content in Figure 13? In fact, the influence may be stated here too, but in a different form. The experiments were here performed for one cylinder at constant speed for each curve, hence jumps do not appear. Different cavitation numbers were obtained by change of pressure, whereby high pressures correspond to high  $R$ . Hence, air content increases with increasing  $R$  and  $C_x$  decreases for  $\sigma = \text{constant}$ ; the influence of air content is expressed by different angles of inclination of the resulting straight lines, the slope decreases with growing  $R$ .

The curves, Figure 13, generally peaking support the reasoning mentioned above. They differ from it for the following reason: Because of the scattering and lack of points these are connected in such a way that curves for greater  $R$  have a greater slope and a greater  $C_x$ , which is strictly contrary to Figure 15. In fact, with constant air content, all points should lie in the same straight line.

We must mention another puzzling point. The lowest curve ( $\sigma = 2.91$ , Figure 14) has the same character as the others, notwithstanding the fact that it represents the subcritical range, where the influence of  $R$  should be overwhelming, which cannot be stated here. Therefore, we must recall a former statement dealing with the normal and cavitating flow in this region: When  $R$  is chosen in a range where  $C_x$  for normal flow is practically constant,  $C_x$  remains also constant in a subcritical cavitating flow. In the present case the interval of  $R$  (200,000 to 800,000) corresponds to a normal flow beyond the "critical" where  $C_x$  no longer depends appreciably upon  $R$ .

The similar character of this curve permits the conclusion that air content has an influence over the whole range of  $\sigma$  for both the subcritical and supercritical regions. It is necessary to extend experiments such as discussed in Figure 14 towards smaller  $R$  including the critical range; then we shall find a sharply pronounced difference between curves corresponding to the subcritical and supercritical ranges of cavitation numbers.

Summarizing, we first point out the tremendous influence of  $R$  in the subcritical range of cavitating flow. But when two experiments have been made in such a range of  $R$  that, for conditions of normal flow, the resistance coefficient  $C_x$  is practically constant, we can neglect the influence of  $R$  on cavitating conditions too.

The latter fact is responsible for the erroneous opinion that the Reynolds number  $R$  has no influence on cavitation phenomena at all.

In the supercritical range of  $\sigma$ ,  $R$  has practically no influence, but it is necessary to perform additional and more accurate experiments when we want to settle this problem in principle.

At first, it seems that these statements suggest the possibility of using only one criterion of similitude, when we confine ourselves to one of the regions of cavitation numbers ("subcritical" or "supercritical," leaving aside the critical region of transition); i.e., to use the equality of cavitation numbers in the supercritical or the equality of Reynolds numbers in the subcritical range. However, that is only possible in the supercritical region. In the subcritical region (as pointed out before) besides the resistance coefficient  $C_x$ , another factor is of primary importance—the erosion; its dependence upon  $R$  and  $\sigma$  has not yet been investigated at all. Hence, for obtaining a complete similarity in the subcritical region, we must at the same time have equal Reynolds and cavitation numbers. In practice it is very difficult to comply with this rule.

Apparently, Reynolds number has an important influence in the subcritical and critical region of cavitation, not only for such bodies as a cylinder but even for streamlined bodies such as blades of turbines and screws.

We may cite here Ackeret:

"Experiments with cavitating models of turbines and pumps are in good agreement with those in full size. Only in the case of one old slow-running turbine with sharp blades having rounded edges, we did not get the expected power in the region of highly developed cavitation. Perhaps in highly-developed cavitation, results cannot be converted from model to full scale."

The last conclusion indicates that Ackeret had not suspected a possible influence of  $R$ ; meanwhile our investigation indicates the possibility of such an effect near the critical  $\sigma$ . However, this problem should be studied further on profiles. The reasons are not yet known for the jump in the  $C_x$  curve at the critical cavitation number. We consider at first the normal flow without cavitation, which can exist under three forms.

1. Viscous flow (very small  $R$ ).
2. Flow with laminar boundary layer
3. Flow with turbulent boundary layer

In the first of the above states, the resistance depends essentially on viscous forces and comparatively little upon pressure distribution. Thus, our method of determining resistance from pressure measurements would be erroneous; accordingly, such experiments were not performed.

The second form of flow, characterized by the laminar boundary layer, leads to separation at a certain point of the surface. The vortices are small and of small intensity. Pressure distributions (Figure 6,  $\sigma = 4.6$  and Figure 7,  $\sigma = 8.91$ ) show that the pressure, after reaching a minimum increases somewhat and then remains nearly constant.

The third kind of flow, characterized by a turbulent boundary layer, presents another picture; the point of separation is moved backwards. Correspondingly, vortices are moved back, too; they increase in size and intensity and cause an important rise of pressure behind the cylinder by creating a flow in the opposite direction. Hence, the coefficient  $C_x$  is decreased in a pronounced way. These statements are clearly supported by the pressure distribution shown in Figure 10,  $\sigma = 12.95$  and Figure 11,  $\sigma = 2.75$ .

When the flow is cavitating, conditions remain the same in the region of large  $\sigma$  (subcritical) up to a certain moment. This can be concluded from the pressure distributions as well as from the  $C_x$  curve, which only differs slightly from the curve of "normal" flow at corresponding  $R$  numbers.

Hence, the form of the cavitating flow in this region is determined by the boundary layer (Reynolds number) in the same way as the form of normal flow.

When the cavitation number  $\sigma$  is decreased below the critical value, a sudden change of pressure distribution in the low pressure zone is caused (turbulent boundary layer, see Figure 10  $\sigma = 1.57$  and 1.55). This change results in a slight increase of pressure above and below the cylinder and an important drop behind it; the distribution of pressure becomes somewhat similar to the distribution valid for a flow with a laminar boundary layer. Thus the jump in the curve  $C_x$  can be explained. The phenomenon develops in the



same way as though experiments were performed in a normal flow, starting with big  $R$  and proceeding gradually to smaller ones. The reason for this pressure change, and consequent change in  $C_x$ , is the separation of the flow from the cylinder and the formation of a stable cavity consisting of air and steam bubbles.

When we consider a flow with a laminar boundary layer, a separation of flow will start, too, at the critical cavitation number, but the pressure distribution is not much changed and hence no jump should occur in the  $C_x$  curve.

Reducing  $\sigma$  still further below the critical value, the pressure coefficient is rising in the underpressure zone, but the character of its distribution is not altered fundamentally for any form of flow. (Some changes, like a shifting of the separation point, can be observed, having only a small influence on  $C_x$ ). That is quite natural, as after separation the problem of boundary layer and of kinds of flow in the earlier sense disappears. We have a new form—the flow of separation.

#### CONCLUSIONS

Notwithstanding the preliminary character of the investigation we may make the following fundamental statements:

1. In the region of large  $\sigma$ , called "subcritical," the kind of flow and consequently  $C_x$  depend almost entirely on  $R$ .
2. In the region of small "supercritical"  $\sigma$ ,  $C_x$  is practically independent of  $R$ .
3. The boundary between the above mentioned regions is the "critical"  $\sigma$ , which corresponds to the moment of separation of the flow and formation of a flow of separation
4. To get similitude in model work or when comparing phenomena we must keep the cavitation number  $\sigma$  constant, provided we know positively that we are restricted to the supercritical region only
5. To obtain similitude in the subcritical range we must at the same time have equal  $\sigma$  and  $R$  numbers.
6. The above mentioned criteria are necessary but not sufficient. There exists another factor influencing  $C_x$  and hence the similitude, which, in our opinion, is the air content; this assumption must be checked.

7. A clear terminology is reached when by cavitation or cavitation flow only such phenomena are denoted which are confined to the subcritical range of  $\sigma$ ; phenomena in the supercritical range, being quite different and not connected with erosion, should be described as flow of separation.

Concluding, we may remark that these deductions are strictly applicable only to such bodies as a cylinder or sphere; but by logical reasoning they are applicable to some degree to other bodies also. Thus, for instance, the critical  $\sigma$  exists for any body; hence the total region of  $\sigma$  when testing any body can be divided into sub- and supercritical zones. With a high degree of probability we can assert that in the supercritical range the influence of  $R$  for any body will be negligibly small. When testing in the subcritical region the influence of  $R$  may vary between wide limits (from preponderant to zero) dependent on the form of body, as may be deduced from the relation mentioned before between normal and cavitating flow. We may even guess the degree of influence: When for the normal flow the influence of  $R$  is small it will be small for the cavitating flow, too, and vice versa.

In studying cavitation phenomena, we should observe these rules and not confine ourselves to an equality of cavitation numbers only in all cases.

MIT LIBRARIES

DUPL



3 9080 02993 0119

